Wigner algebra as a tool for the design of achromatic optical processing systems

Dayong Wang
Avi Pe'er
Adolf W. Lohmann, MEMBER SPIE
Asher A. Friesem, MEMBER SPIE
Weizmann Institute of Science
Department of Physics of Complex Systems
Rehovot 76100, Israel
E-mail: avi.peer@weizmann.ac.il

Abstract. Achromatic optical processing systems can perform a variety of operations with temporally incoherent (polychromatic) light, without color blurring. The system design is a complicated task, since usually the scale at the output depends on the wavelength. The design goal is to eliminate this scale dependence as well as two other wavelength-dependent defects. Such a goal is generally achieved by modifying lens design procedures. Here we do it in a different manner. Specifically, we resort to matrix algebra, applied to the Wigner distribution function. The resulting Wigner matrix includes elements that characterize wavelength-dependent parameters of the optical systems. Such a characterization provides a clear insight into what is needed to reduce the wavelength dependence, and indeed achieve the achromatization of the systems. This design approach is valid with either wave optics or geometrical optics. The basic principles and specific design examples of achromatic optical Fourier transformers and Fourier processing systems with low chromatic aberrations over the entire visible spectrum are presented.
 [S0091-3286(00)02311-4]

Subject terms: achromatic processing systems; Wigner distribution function; achromatic Fourier transformations; spatial filtering.

Paper 990494 received Dec. 13, 1999; revised manuscript received June 27, 2000; accepted for publication June 27, 2000.

1 Introduction

Optical information-processing and optical computing systems benefit from high computational speed and a high degree of inherent parallelism. Usually these systems employ monochromatic coherent light sources such as lasers, so they suffer from high sensitivity to optical setup noise (dust, scratches, and fingerprints on optical surfaces) and to alignment errors of the optical components. The use of polychromatic light for optical signal processing, either spatially coherent or spatially incoherent, can reduce these problems.[1–11] Indeed, the use of polychromatic light has been effectively exploited in a number of applications.[12–21] Unfortunately, a basic problem arises with polychromatic light, and that is chromatic dispersion (wavelength dependence) at the output.

Several design methods have been proposed to reduce the wavelength dependence of various optical processing systems. Some, by Leith and Swanson,[3] Morris and Georgle,[4] and Collins,[7] did so in the context of holography, where the achromatization is achieved with either wavelength-compensating diffractive gratings or zone plates. Alternatively, a combination of diffractive zone plates and achromatic refractive lenses can be used. For example, Katyl[1] proposed an achromatic Fourier transform and spatial-filtering arrangement consisting of two zone plates and a cemented achromat. Morris[5,6] studied theoretically an achromatic Fourier transform system (AFS) formed by a cascade of three compound elements, each combining an adjacently spaced chromat and a zone lens. Ferriere and Goedgebuer[8] and also Leon and Leith[9] achieved an achromatic Fourier transform with two zone plates and two dispersive lenses. More recently, Andrés et al.[12,13,16,18] developed an AFS having low chromatic aberrations with three elements. Also, a general solution and a special case for broadband imaging systems with a combination of three dispersive lenses has been obtained by Faklis and Morris.[11] Tajahuerce et al.[19] presented an achromatic optical processing architecture with broadband point-source illumination. Most of these design methods are based on either geometrical optics considerations or paraxial Fresnel diffraction theory.

In this paper, we propose to design achromatic processing systems by exploiting the Wigner algebra, namely, matrix-vector multiplication applied to the coordinates of the Wigner distribution function (WDF). The WDF was introduced into information optics by Bastiaans[22,23] and recently reviewed by Dragoman[24] and Lohmann et al.[25,26] Lancis et al.[14] have applied the WDF to achromatize self-imaging phenomenon. Here we develop a Wigner matrix formulation to achieve a variety of achromatization with first-order and second-order approximations. The final results are obtained with simple matrix multiplication and direct operation on each element of the total matrix. They are well suited for computer calculation and can provide a clear physical insight and interpretation. Moreover, the WDF algebra is a valid tool for the analysis and synthesis of optical systems based on either wave optics or geometrical optics.

In Sec. 2, we briefly review the WDF matrix formalism for monochromatic light and its relationship with linear canonical transforms. In Sec. 3, we describe its generalization to polychromatic light, and as a consequence, the statement

of the design goal: *achromatization* in ''Wigner language.'' In Sec. 4, the analysis and some design examples of achromatic Fourier systems are presented. In Sec. 5, we demonstrate the design of a white-light spatial filtering system with spatially coherent light. Finally, some concluding remarks are given in Sec. 6.

2 Wigner Algebra for Optical Systems with Monochromatic Light

Every complex amplitude distribution $u(x,y)$ or signal $u(t)$ can be described indirectly but uniquely by a Wigner distribution function. For the sake of simplicity, one-dimensional notation is used for $u(x)$, but generalization to two dimensions is straightforward. The WDF is a mathematical operation applied to the input field distribution $u(x)$ in two equivalent forms, given by

$$W(x,v)=\int_{-\infty}^{\infty} u\left(x+\frac{x'}{2}\right)u^*\left(x-\frac{x'}{2}\right)\exp(-j2\pi vx')\,\mathrm{d}x', \tag{1a}$$

$$W(x,v)=\int_{-\infty}^{\infty} \tilde{u}\left(v+\frac{v'}{2}\right)\tilde{u}^*\left(v-\frac{v'}{2}\right)\exp(j2\pi v'x)\,\mathrm{d}v', \tag{1b}$$

where v is the spatial frequency, the asterisk * means complex conjugation, and

$$\tilde{u}(v)=\int_{-\infty}^{\infty} u(x)\exp(-j2\pi vx)\,\mathrm{d}x. \tag{2}$$

The transformation from $u(x)$ to $W(x,v)$ is reversible, apart from an irrelevant constant phase factor, so

$$\int_{-\infty}^{\infty} W\left(\frac{x}{2},v\right)\exp(j2\pi vx)\,\mathrm{d}v=u(x)u^*(0), \tag{3a}$$

$$\int_{-\infty}^{\infty} W\left(x,\frac{v}{2}\right)\exp(-j2\pi vx)\,\mathrm{d}x=\tilde{u}(v)\tilde{u}^*(0). \tag{3b}$$

Consider now an input signal $u_1(x_0)$ that is modified to $u_2(x)$ by a first-order optical system. In the space domain, this modification of the input signal by the optical system can be described by a linear canonical transformation[27–32] (sometimes called the ''generalized Huygens'' or ''Fresnel transformation''), written as

$$u_2(x)=\int_{-\infty}^{\infty} u_1(x_0)h(x;x_0)\,\mathrm{d}x_0, \tag{4}$$

where the kernel $h(x;x_0)$ is

$$h(x;x_0)=\begin{cases}\dfrac{1}{\sqrt{jB}}\exp\left[\dfrac{j\pi}{B}(Ax_0^2+Dx^2-2xx_0)\right], & B\neq 0,\\ \dfrac{1}{\sqrt{A}}\exp\left[j\dfrac{\pi C}{A}x^2\right]\delta\left(x_0-\dfrac{x}{A}\right), & B=0,\end{cases} \tag{5}$$

where B is identified as the scaling factor of the transformation and we have ignored constant phase factors. Any linear canonical transform is completely specified by its parameters A, B, C, and D, which construct a 2×2 unimodular transformation.

The relationship between the Wigner function $W_1(x_0,v_0)$ of $u_1(x_0)$ and the Wigner function $W_2(x,v)$ of $u_2(x)$ can be found by inserting the canonical transform integral of Eq. (4) into the WDF representation, to yield

$$W_2(x,v)=W_1(Dx-Bv,-Cx+Av). \tag{6}$$

This equation suggests that the effect of modifying $u_1(x_0)$ to $u_2(x)$ by the linear canonical transformation (4) is equivalent to a coordinate transformation of $W_1(x_0,v_0)$ into $W_2(x,v)$. This transformation can be described as a vector-matrix product, which relates the input variables (x_0,v_0) to the output variables (x,v), as

$$\begin{pmatrix}x\\ v\end{pmatrix}=\begin{bmatrix}A & B\\ C & D\end{bmatrix}\begin{pmatrix}x_0\\ v_0\end{pmatrix}. \tag{7}$$

We refer to the 2×2 matrix in Eq. (7) as the Wigner matrix. For analyzing and synthesizing optical systems, the matrix approach of the Wigner representations is convenient and has some advantageous properties. For example, if several optical configurations are cascaded, the Wigner matrix of the overall system can be found by multiplication of the matrices of the individual transformation configurations. In this way, the extensive use of complicated chirp integrals is no longer needed in the optical design. Also, both the field distribution and its spatial-frequency spectrum can be obtained immediately from the phase-space presentation [Eqs. (3a) and (3b)].

More important is that with the help of Eqs. (4), (5), and (7) it is possible to gain an insight into the role of each element in a Wigner matrix. This insight can generally be demonstrated for two cases when $B\neq 0$ and $B=0$:

1. When $B\neq 0$, the parameter A affects the quadratic phase factor at the input plane, while D affects the quadratic phase factor at the output plane. Element B is the total scaling factor of the overall system. If now $A=0$, then the overall system serves as Fourier-transformation system, where D/B equals the quadratic phase factor at the output Fourier plane. Furthermore, if $D=0$ at the same time, the output Fourier transform does not include any quadratic phase factor.
2. When $B=0$, the overall system serves as an imaging system. Then A represents the magnification of the overall system, while C/A corresponds to the quadratic phase factor at the output plane.

For future reference, we list the correspondence between some basic processes of physical optics and their Wigner matrix counterparts. Assuming that the wavelength of the illumination light is λ, then free-space propagation over a distance z corresponds to

$$\begin{bmatrix} 1 & \lambda z \\ 0 & 1 \end{bmatrix}, \tag{8}$$

refractive achromatic lens with a focal length f corresponds to

$$\begin{bmatrix} 1 & 0 \\ -1/\lambda f & 1 \end{bmatrix}, \tag{9}$$

and a diffractive lens (Fresnel zone plate) corresponds to

$$\begin{bmatrix} 1 & 0 \\ -1/\lambda_0 f_0 & 1 \end{bmatrix}, \tag{10}$$

where $\lambda_0 f_0 = R^2/2$, R is the radius of the innermost ring of the diffractive lens, and f_0 is the focal length at the designed wavelength λ_0. In addition, the ideal Fourier transformation corresponds to

$$\begin{bmatrix} 0 & b \\ -1/b & 0 \end{bmatrix}, \tag{11}$$

where b is the total scaling factor. If the equivalent focal length of the overall optical system is f, then $b = \lambda f$. For a zone plate, the scaling factor b is now $R^2/2$. Finally, an ideal magnifier corresponds to

$$\begin{bmatrix} M & 0 \\ 0 & 1/M \end{bmatrix}, \tag{12}$$

and a fractional Fourier transformation corresponds to

$$\begin{bmatrix} \cos\phi & b\sin\phi \\ -\sin\phi/b & \cos\phi \end{bmatrix}, \tag{13}$$

where b is the total scaling factor and the angle ϕ is related to the fraction p of the Fourier transformation by $\phi = p\pi/2$.

3 Generalization to Polychromatic Light and Design Goal

In the preceding section we showed that each element of the Wigner matrix signifies a different operation of the optical system. Special significance ensues when one of the elements is zero. Indeed, the aim of a particular system design is often synonymous with forcing one of the four Wigner matrix elements to be zero. That is the spirit of the following two sections, which deal with the design of polychromatic optical processing systems.

With polychromatic light, it is usually necessary to overcome three problems during the system design: a wavelength-dependent lateral scaling factor at the output plane, wavelength-dependent longitudinal location $z(\lambda)$ of the output, and a wavelength-dependent quadratic phase factor at the output. In general, the location of the output plane is fixed, so we need only deal with wavelength-dependent scaling factor and quadratic phase factor. Sometimes, when we are interested only in the intensity at the output, even the quadratic phase factor problem is eliminated. Thus, we are mainly concerned to achieve one output at a fixed plane, which is an incoherent superposition of many suboutputs each of a different wavelength but all of the same lateral scale.

Since the Wigner matrix includes inherently the wavelength dependence of the transformation, it should, in principle, be possible to design an achromatic optical system by requiring that the relevant elements in the matrix be wavelength-independent. Such a requirement can be fulfilled by changing the optical and geometrical parameters of the optical components in the system. As an example, for an ideal achromatic Fourier transformation the relevant elements of the Wigner matrix must be $A(\lambda) = D(\lambda) = 0$ and $\partial B/\partial\lambda = 0$. The demand for exact chromatic correction will lead to constraints on the dispersion characteristics of the optical components, requiring all wavelengths to behave in the same specific manner. Sometimes these dispersion constraints are impractical and approximations are required.

4 Achromatic Fourier Transformations

For monochromatic light, the Wigner matrix of an optical system that can perform a perfect Fourier transformation is characterized by $A = D = 0$. When $A = 0$ and $D \neq 0$, the Fourier transformation is imperfect, in that additional quadratic phase terms exist in the output distribution. Such an imperfect Fourier transformation is adequate in those applications where only the intensity (power spectrum) is needed. If, in addition, the scaling factor B is independent of wavelength, at least to the first-order approximation, then the Fourier transformation is achromatized. Adjusting this coefficient B is the central task ahead of us.

4.1 *Imperfect Achromatic Fourier Transformations*

An imperfect achromatic Fourier transformation could be performed with two zone plates and one refractive achromatic lens.[8,9] So we will start from such a three-component system of one refractive achromatic lens and two dispersive lenses.

In order to obtain an achromatic Fourier transformation, it is necessary to correct the chromatic dispersion of the scaling factor $B(\lambda)$, while requiring $A(\lambda) = 0$. Usually, it is impractical to satisfy these requirements completely. So we must consider the first-order and second-order approximations. There are two approaches to make approximations. In one, the elements $A(\lambda)$ and $B(\lambda)$ are directly approximated in the total Wigner matrix of the transformation system. In the other approach, first an ideal theoretical solution is obtained by using the Wigner matrix, and then this theoretical solution is approximated with practical optical components. The second approach is computationally more convenient for higher-order approximations.

4.1.1 *First-order approximation solution*

Let us consider the optical setup shown in Fig. 1, where the two dispersive lenses ZP_1 and ZP_2 are simple zone plates, and the refractive lens L_1 is an achromat. We call this kind of optical setup a type-I achromatic Fourier transformer. Assuming that the input object is illuminated by a parallel beam of spatially coherent white light, then the total Wigner matrix of the transformation system can be obtained, by cascading seven matrices, as

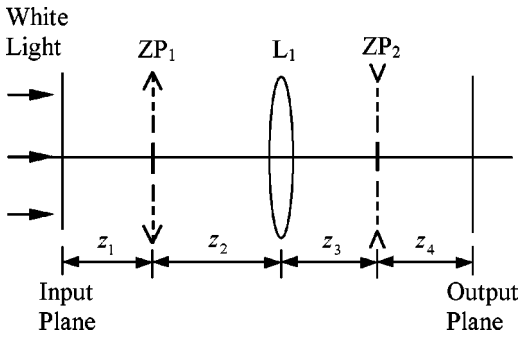

Fig. 1 Setup (type I) for performing an imperfect achromatic Fourier transform.

$$\begin{bmatrix} A(\lambda) & B(\lambda) \\ C(\lambda) & D(\lambda) \end{bmatrix} = \begin{bmatrix} 1 & \lambda z_4 \\ 0 & 1 \end{bmatrix} \begin{bmatrix} 1 & 0 \\ -\dfrac{1}{\lambda_0 f_{02}} & 1 \end{bmatrix} \begin{bmatrix} 1 & \lambda z_3 \\ 0 & 1 \end{bmatrix} \times \begin{bmatrix} 1 & 0 \\ -\dfrac{1}{\lambda f_1} & 1 \end{bmatrix} \begin{bmatrix} 1 & \lambda z_2 \\ 0 & 1 \end{bmatrix} \begin{bmatrix} 1 & 0 \\ -\dfrac{1}{\lambda_0 f_{01}} & 1 \end{bmatrix} \times \begin{bmatrix} 1 & \lambda z_1 \\ 0 & 1 \end{bmatrix}, \tag{14}$$

where f_{01} and f_{02} are the focal lengths of ZP_1 and ZP_2 for the wavelength λ_0, respectively, and f_1 is the focal length of L_1.

In a first-order approximation, the achromatic correction of the scaling factor will be achieved if the derivative of the function $B(\lambda)$ vanishes at a certain wavelength λ_0 at the center of the spectrum. Also, since the condition for Fourier transformation is satisfied to first order if both the function $A(\lambda)$ and its derivative are equal to zero at the wavelength λ_0, then the values of $B(\lambda)$ and $A(\lambda)$ are almost stationary. In mathematical terms, we require

$$A(\lambda)\big|_{\lambda=\lambda_0} = 0, \tag{15a}$$

$$\left.\frac{\partial A(\lambda)}{\partial \lambda}\right|_{\lambda=\lambda_0} = \left.\frac{\partial B(\lambda)}{\partial \lambda}\right|_{\lambda=\lambda_0} = 0. \tag{15b}$$

After some algebraic manipulations, which can be done easily by a personal computer, Eqs. (15) lead to the constraints

$$z_3^2 = -f_{01} f_{02}, \tag{16a}$$

$$z_3 = f_1, \tag{16b}$$

$$z_4 = \frac{z_3^2}{z_2 - z_3 - 2f_{01}}. \tag{16c}$$

Equations (16) indicate that the focal lengths of ZP_1 and ZP_2 must be of opposite signs and the focal length f_1 of the refractive achromatic lens L_1 must be positive and equal to the distance z_3 between this lens and the second zone plate. The distance z_3 depends only on the focal lengths of the two zone plates. Furthermore, we must satisfy the geometrical constraints $z_1>0$, $z_2>0$, and $z_3>0$ in order to obtain the proper sequence of components in the optical system. It is possible to predict the positions of the output Fourier plane for two configurations: (1) $f_{01}<0$ and $f_{02}>0$, and (2) $f_{01}>0$ and $f_{02}<0$. In practice, it is desirable to obtain a real, rather than virtual, achromatic Fourier transformation, i.e., $z_4>0$. So, according to Eq. (16c), if the same z_4 and z_3 are used in the two configurations, then the distance z_2 in the first configuration is much shorter than in the second. This results in a more compact optical system for the first configuration.

Under the constraints in Eqs. (16), $A(\lambda)$ and $B(\lambda)$ become

$$A(\lambda) = -\frac{z_4}{|f_{01} f_{02}|^{1/2}} \frac{(\lambda-\lambda_0)^2}{\lambda_0^2} \tag{17}$$

and

$$B(\lambda) = -\frac{z_1 z_4}{|f_{01} f_{02}|^{1/2}} \frac{\lambda(\lambda-\lambda_0)^2}{\lambda_0^2} \pm z_4 \left|\frac{f_{01}}{f_{02}}\right|^{1/2} \frac{\lambda(2\lambda_0-\lambda)}{\lambda_0}, \tag{18}$$

where the + sign corresponds to the first configuration and the − sign to the second configuration.

In order to assess the achromatic correction, we introduce a relative scaling error SE(λ), defined as

$$\mathrm{SE}(\lambda) \equiv \frac{B(\lambda)-B(\lambda_0)}{B(\lambda_0)} = \frac{(\lambda-\lambda_0)^2}{\lambda_0^2}\left(\mp\frac{z_1}{|f_{01}|}\frac{\lambda}{\lambda_0}-1\right), \tag{19}$$

where the − sign corresponds to the first configuration and the + sign to the second configuration. Such a relative scaling error is especially important in assessing the output correlation of a Vander Lugt optical correlator, which requires, as a rule of thumb, that it be less than 5%.

Now by substituting the total Wigner matrix of Eq. (14) into Eq. (7), the physical coordinate x of the output plane can be obtained as

$$x = A(\lambda)x_0 + B(\lambda)v_0, \tag{20}$$

where x_0 is the coordinate in the input plane and v_0 is the spatial frequency coordinate of the input object. Ideally, $A(\lambda)$ should be zero and $B(\lambda)$ should be constant, in order to obtain an exact achromatic Fourier transformation. In practice, however, there is transverse blurring at the Fourier transform output plane. For a given input object, Eq. (20) shows that the transverse blurring arises from two sources. One is $A(\lambda)$, which is usually referred to as a defocus chromatic aberration. Since it has a nonzero value (except at wavelength λ_0), the same spatial frequency components at different parts of the input object will not coincide at the same point in the output Fourier plane. Thus $A(\lambda)$ effectively determines the highest resolution in the output Fourier plane as a function of the input object size. The effect

of defocusing by $A(\lambda)$ is uniform over the output plane. For a given wavelength, it is possible to define a maximum transverse aberration, as

$$\Delta x_{\mathrm{TDA}}(\lambda)=|A(\lambda)|\,\Delta x_0, \tag{21}$$

where Δx_0 is the size of the input object, whose center coincides with the optical axis.

Another source of transverse blurring is $B(\lambda)$, which is referred to as transverse chromatic aberration. For a given spatial frequency, the maximum transverse chromatic aberration is

$$\Delta x_{\mathrm{TCA}}=|B(\lambda_0)|\,(\mathrm{SE}_{\max}-\mathrm{SE}_{\min})\,|v_0|, \tag{22}$$

where $\mathrm{SE}_{\max}$ and $\mathrm{SE}_{\min}$ are the maximum and minimum values of the relative scaling error $\mathrm{SE}(\lambda)$ given in Eq. (19). Thus $B(\lambda)$ effectively determines the maximum spatial frequency component at the input object that can be transformed properly. In other words, the variations in $B(\lambda)$ reduce the resolution at the higher spatial-frequency locations of the output plane. Accordingly, it is possible to quantitatively assess the transverse blurring when the size and the highest spatial-frequency component of the input object are given, and when the spectral distribution of the source is specified.

A main goal of the design is to minimize $|A(\lambda)|$ and $|\mathrm{SE}(\lambda)|$ by properly selecting the parameters λ_0, f_{01}, f_{02}, z_1, and z_4 (or z_2). Yet, from a practical point of view, it is desired that the optical setup be compact and that the scaling factor $B(\lambda_0)$ of the Fourier transformation be large. According to Eqs. (17) to (19), these requirements cannot be satisfied simultaneously. Specifically, $A(\lambda)$ varies as λ^2, but $B(\lambda)$ and $\mathrm{SE}(\lambda)$ vary as λ^3. When the distance z_1 to the input object is very small (compared with the focal length f_{01}), then $B(\lambda)$ and $\mathrm{SE}(\lambda)$ display parabolic behavior around λ_0. Indeed, when $z_1=0$, then $B(\lambda)$ and $\mathrm{SE}(\lambda)$ are exact parabolas in λ. The designed wavelength λ_0 is usually chosen as $\lambda_0=(\lambda_{\min}+\lambda_{\max})/2$, where $\lambda_{\min}$ and $\lambda_{\max}$ denote the two extreme wavelengths of the incident light. Typically, we deal with the full visible wavelength range, where $\lambda_{\min}=0.4\,\mu$m and $\lambda_{\max}=0.7\,\mu$m, so $\lambda_0=0.55\,\mu$m. In this way, $A(\lambda_{\min})=A(\lambda_{\max})$. For the other parameters, some compromise must be made.

Since a solution exists for any choice of the distances z_1 and z_2, it is possible to let both distances be zero (i.e., $z_1=z_2=0$) and interchange the order of the first zone plate and the achromatic lens. Such an interchange leads to another type of optical setup for performing the achromatic Fourier transformation. In this setup, a color-blurred Fourier transform is formed at the back focal plane of the achromatic lens L_1. This Fourier transform is then imaged by two zone plates ZP_1 and ZP_2 so as to have the same size at the same plane for all wavelengths. The new optical setup, which we call the type-II achromatic Fourier transformer, is shown in Fig. 2. The symbols have the same meanings as in Fig. 1.

Following the procedure as for the type-I Fourier transformer setup, we can obtain the total Wigner matrix. With the same requirements as in Eqs. (15), we then obtain the same constraint for z_3 as in Eq. (16a). Thus the focal lengths of the two zone plates still must have opposite signs. But the distance z_4 and the focal length f_1 are now

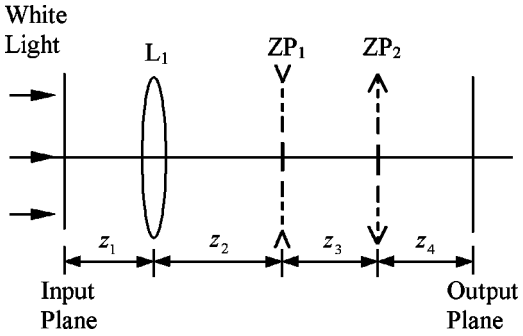

Fig. 2 Setup (type II) for performing an imperfect achromatic Fourier transform.

$$z_4=\frac{f_{02}}{2\mp R_{21}^{1/2}}, \tag{23}$$

$$f_1=z_2+z_3, \tag{24}$$

where the $-$ sign corresponds to a configuration with $f_{01}<0$ and $f_{02}>0$, the $+$ sign to a configuration with $f_{01}>0$ and $f_{02}<0$, and R_{21} is the ratio $|f_{02}/f_{01}|$. We note that z_4 depends only on the focal lengths of the two zone plates. Furthermore, in the first configuration ($f_{01}<0$ and $f_{02}>0$), z_4 is positive for R_{21} in the interval [0, 4], and negative for R_{21} greater than 4. In the other configuration, z_4 is always negative. Comparing Eqs. (24) with Eqs. (16b), we find that, in both type-I and type-II optical setups, it is necessary to position the second zone plate ZP_2 at the back focal plane of the refractive achromatic lens L_1.

Next we consider in more detail the transverse blurring in the configuration with $f_{01}<0$ and $f_{02}>0$. Under the constraints given in Eqs. (16a), (23), and (24), $A(\lambda)$ and $B(\lambda)$ become

$$A(\lambda)=\frac{f_{02}}{f_1(R_{21}^{1/2}-2)}\,\frac{(\lambda-\lambda_0)^2}{\lambda_0^2}, \tag{25}$$

$$B(\lambda)=\frac{1}{R_{21}^{1/2}-2}\left[\left(-f_1R_{21}^{1/2}+f_{02}-\frac{z_1f_{02}}{f_1}\right)\frac{(\lambda-\lambda_0)^2}{\lambda_0^2}+f_1\frac{\lambda(2\lambda_0-\lambda)}{\lambda_0}\right]. \tag{26}$$

Also, we obtain the relative scaling error as

$$\mathrm{SE}(\lambda)=\frac{\lambda(\lambda-\lambda_0)^2}{\lambda_0^3}\left[-R_{21}^{1/2}+\frac{f_{02}}{f_1^2}(f_1-z_1)-\frac{\lambda_0}{\lambda}\right]. \tag{27}$$

Now even if the distance to the input object $z_1=0$, the functions $B(\lambda)$ and $\mathrm{SE}(\lambda)$ no longer display parabolic behavior in λ. Also, larger f_1 will result in a smaller $|A(\lambda)|$

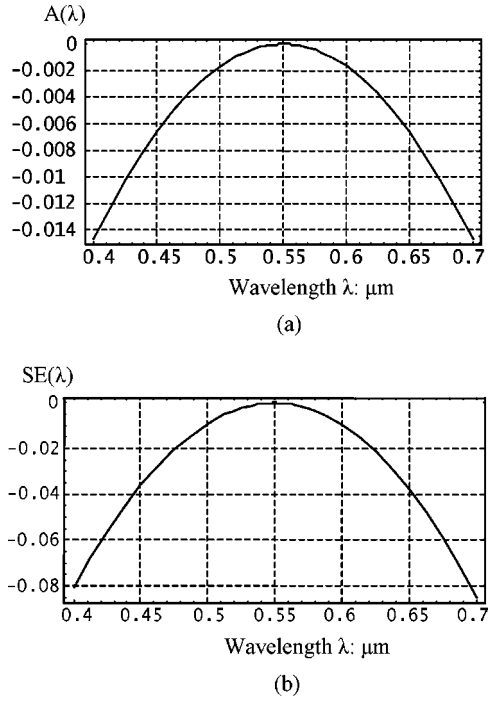

Fig. 3 (a) Defocus chromatic aberrations and (b) relative scaling error as a function of the wavelength under the first-order approximation.

and a larger scaling factor $|B(\lambda)|$. Note, however, that if $z_1 < f_1$, any increase of f_1 will increase $|\mathrm{SE}(\lambda)|$ as well. So some compromise is necessary.

Finally we consider a specific design, whereby $z_1 = 0$, so the input object is adjacent to the achromatic lens L_1. In such an optical setup, the input object is essentially illuminated with a spherical wave converging to the center of the second zone plate ZP_2. With the spherical-wave illumination, it is possible to alter the scaling factor of the Fourier transform simply by moving the input object along the optical axis. Such a setup has been recently studied by Tajahuerce et al.[18] In our design, the focal length of ZP_1 was -55 cm and the focal length of ZP_2 was 10 cm, both at the wavelength $\lambda = 0.514\,\mu$m; and $f_1 = 30$ cm, $z_2 = 8.08$ cm, $z_3 = 21.92$ cm, and $z_4 = 5.94$ cm. The resulting defocus aberration $A(\lambda)$ and relative scaling error $\mathrm{SE}(\lambda)$ are shown in Fig. 3. As shown, the maximum $|A(\lambda)|$ is 0.0145, and the maximum relative scaling error $|\mathrm{SE}(\lambda)|$ is about 8%. The equivalent focal length of the overall optical transformation setup is about 19 cm at the wavelength λ_0, where its total length is 35.94 cm. It should be noted that the maximum $|A(\lambda)|$ could be improved by a factor 2 if we tuned the parabola $A(\lambda)$ to have two zero points. That would mean replacing the requirement in Eq. (15a) with $A(\lambda_0) = -A(\lambda_{\min})$.

4.1.2 *Second-order approximation solution*

For a second-order approximation, it is necessary to replace at least one of the relatively simple zone plates with an element that has more general dispersive properties. This is shown in the optical setup of Fig. 4, where ZP_2 of the original type-I optical setup was replaced by a general dispersive element L_2, and $z_1 = 0$. If we let L_2 be an ideal dispersive component with a required exact optical power $\Phi_{\mathrm{ideal}}(\lambda)$, and place it at the back focal plane of lens L_1, then the total Wigner matrix of the optical setup is

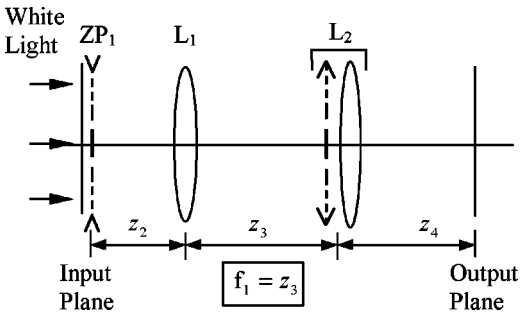

Fig. 4 Setup (type I) for performing an imperfect achromatic Fourier transformation to higher-order approximation. The required ideal optical power of lens L_2 is $\Phi_{\mathrm{ideal}}(\lambda)$.

$$\begin{bmatrix} A(\lambda) & B(\lambda) \\ C(\lambda) & D(\lambda) \end{bmatrix} = \begin{bmatrix} 1 & \lambda z_4 \\ 0 & 1 \end{bmatrix} \begin{bmatrix} 1 & 0 \\ -\dfrac{\Phi_{\mathrm{ideal}}(\lambda)}{\lambda} & 1 \end{bmatrix} \begin{bmatrix} 1 & \lambda f_1 \\ 0 & 1 \end{bmatrix} \times \begin{bmatrix} 1 & 0 \\ -\dfrac{1}{\lambda f_1} & 1 \end{bmatrix} \begin{bmatrix} 1 & \lambda z_2 \\ 0 & 1 \end{bmatrix} \times \begin{bmatrix} 1 & 0 \\ -\dfrac{1}{\lambda_0 f_{01}} & 1 \end{bmatrix}. \tag{28}$$

For an imperfect achromatic Fourier transform, the ideal theoretical solution could be obtained if $A(\lambda)$ and $B(\lambda)$ in Eq. (28) fulfilled the conditions

$$A(\lambda) = 0, \tag{29a}$$

$$\frac{\partial B(\lambda)}{\partial \lambda} = 0. \tag{29b}$$

For the optical setup in Fig. 4, we only need solve Eq. (29a) to obtain $\Phi_{\mathrm{ideal}}(\lambda)$, and then Eq. (29b) is satisfied automatically. The solution yields the ideal theoretical power $\Phi_{\mathrm{ideal}}(\lambda)$, as

$$\Phi_{\mathrm{ideal}}(\lambda) = \frac{1}{f_1} - \frac{z_2}{f_1^2} + \frac{1}{z_4} + \frac{\lambda_0 f_{01}}{f_1^2}\frac{1}{\lambda}, \tag{30}$$

Unfortunately, a general dispersive lens with the ideal optical power of Eq. (30) is not practical, so we must resort to some approximation. A good approximation is to replace the general dispersive lens L_2 with a hybrid dispersive lens consisting of a zone plate ZP_2 in cascade with a single glass lens. When the plate and the lens are thin, the optical power of the hybrid lens is the sum of the powers of the individual elements. The hybrid dispersive lens can be realized, to a second-order approximation, by requiring that its optical

power $\Phi_{\text{real}}(\lambda)$ be equal to the ideal optical power $\Phi_{\text{ideal}}(\lambda)$ at three different wavelengths λ_1, λ_2, and λ_3. Specifically, let

$$\Phi_{\text{ideal}}(\lambda_m)=\Phi_{\text{real}}(\lambda_m), \quad m=1,2,3, \tag{31}$$

with

$$\Phi_{\text{real}}(\lambda)=\frac{\lambda}{\lambda_0 f_{02}}+c_A[n(\lambda)-1], \tag{32}$$

where $n(\lambda)$ denotes the index refraction of the glass, c_A is a parameter associated with surface curvature of the thin glass lens (i.e., $c_A=1/R_1-1/R_2$ with R_1 as the radius of curvature of the left-hand surface of the lens and R_2 as the radius of curvature of its right-hand surface), and f_{02} is the focal length of ZP_2 at the wavelength λ_0. Equation (31) is equivalent to requiring $A(\lambda)$ to have three zero points in the visible range. The three wavelengths usually should be determined by minimizing the mean squared error function $\overline{[A(\lambda)]^2}$ or $\overline{[\text{SE}(\lambda)]^2}$.

In order to obtain a glass lens with practical geometrical dimensions, it is best to use highly dispersive glass. We chose the glass of type SF6 from Schott, having a known $n(\lambda)$. Also, we chose the three relevant wavelengths as 0.41245, 0.67165, and 0.51805 μm. Then, we solved Eqs. (31) simultaneously and determined uniquely c_A, z_3, and the relations between z_2 and z_4. The results are

$$c_A=-\frac{2.85294}{f_{02}}, \tag{33a}$$

$$z_3^2=-0.638638 f_{01} f_{02}, \tag{33b}$$

$$z_4=\frac{z_3^2}{z_2-z_3-0.143617 f_{01}}. \tag{33c}$$

In accordance with Eqs. (33), c_A is completely determined by the second zone plate, while the optical powers of the additional dispersive glass lens and the second zone plate must have opposite signs. Furthermore, comparing Eqs. (16b) and (16c) with Eqs. (33b) and (33c), we find differences that arise from many orders that are included in the dispersion of the glass lens. For the same reason, when $z_2=0$, it is almost always impractical to achieve a real Fourier transform pattern ($z_4>0$).

It is important to note that the relations in Eqs. (33) are representative of other optical setups, as long as the chosen three wavelengths and the type of glass of the additional dispersive glass lens are same. Also, the tuning needed to optimize this optical setup is the same as for the setup with first-order approximation.

Finally, we present a specific optical setup design with second-order approximation, as shown in Fig. 5. For this design, the relevant parameters are as follows: the focal lengths of the two zone plates are 16 and -16 cm at the wavelength $\lambda=0.633\,\mu$m; $f_1=30$ cm, $c_A=+15.5\,\text{m}^{-1}$, $z_3=14.72$ cm, and $z_4=-12.47$ cm; and we let $z_2=0$ in Eq. (33c). For this optical setup design, $A(\lambda)$ and $\text{SE}(\lambda)$ as functions of wavelength are presented in Fig. 6. As evident, $A(\lambda)$ is bounded by $|A(\lambda)|<0.003$, and the relative scaling error is bounded by $|\text{SE}(\lambda)|<0.5\%$. The equivalent focal length of the overall transformation system is 34 cm at the wavelength 0.5145 μm.

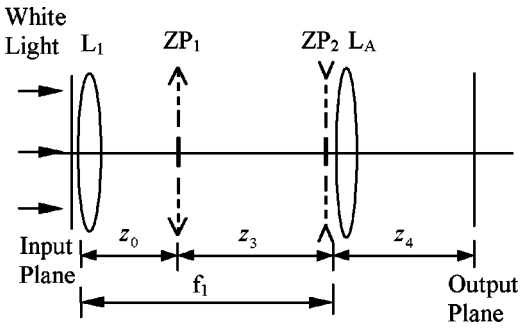

Fig. 5 Setup (type II) for performing an imperfect achromatic Fourier transformation to higher-order approximation.

4.2 *Perfect Achromatic Fourier Transformations*

To modify our earlier designs of imperfect achromatic Fourier transformers so they can perform perfect achromatic Fourier transformation, we need to remove the quadratic phase factor at the output plane. The quadratic phase factor is characterized by the fourth element $D(\lambda)$ in the Wigner matrix. Our approach is to add some lenses at the output Fourier plane of an imperfect achromatic Fourier transformer. This has the advantage that it does not change anything else but the quadratic phase factor at the output plane.

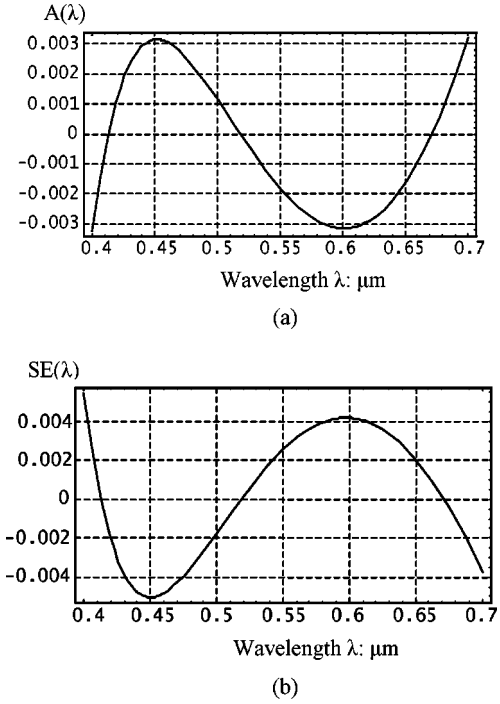

Fig. 6 (a) Defocus chromatic aberrations and (b) relative scaling error as functions of the wavelength under the second-order approximation.

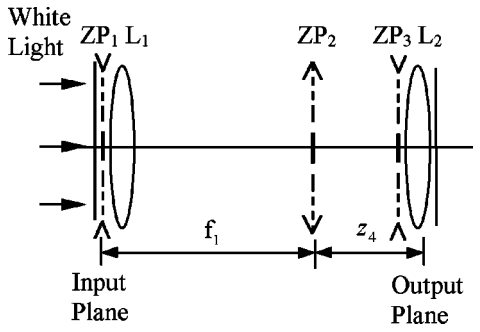

Fig. 7 Compact setup for performing a perfect achromatic Fourier transformation to first-order approximation.

Let us consider the optical setup shown in Fig. 7, which is based on the compact imperfect achromatic Fourier transformer shown in Fig. 1, with $z_1=z_2=0$. We use the combination of a refractive achromatic lens L_2 with a focal length f_2 and a zone plate ZP_3 with a focal length f_{03} at the wavelength λ_0 to compensate for the quadratic phase factor at the output plane. The Wigner matrix for the perfect achromatic Fourier transformation can be obtained by

$$\begin{bmatrix} a(\lambda) & b(\lambda) \\ c(\lambda) & d(\lambda) \end{bmatrix}_{\text{perfect}} = \begin{bmatrix} 1 & 0 \\ -\dfrac{1}{\lambda f_2} & 1 \end{bmatrix} \begin{bmatrix} 1 & 0 \\ -\dfrac{1}{\lambda_0 f_{03}} & 1 \end{bmatrix} \times \begin{bmatrix} A(\lambda) & B(\lambda) \\ C(\lambda) & D(\lambda) \end{bmatrix}_{\text{imperfect}}. \tag{34}$$

The two elementary matrices, which describe the diffractive and the refractive lens in close contact, can be combined, with $-1/\lambda f_2 - 1/\lambda_0 f_{03}$ as lower left coefficient. Then $A(\lambda)$ and $B(\lambda)$ are unchanged, where $a(\lambda)=A(\lambda)$ and $b(\lambda)=B(\lambda)$. Only $C(\lambda)$ and $D(\lambda)$ are affected.

Since the compensation is applied to the output of the compact imperfect achromatic Fourier transformer, the requirement on $d(\lambda)$, similar to that on $A(\lambda)$, is now

$$d(\lambda)|_{\lambda=\lambda_0} = \left.\frac{\partial d(\lambda)}{\partial \lambda}\right|_{\lambda=\lambda_0} = 0. \tag{35}$$

After solving Eq. (35), we obtain the new constraints

$$f_2 = z_4 = \frac{f_{02}}{2 - R_{21}^{1/2}}, \tag{36a}$$

$$f_{03} = -\frac{z_4^2}{f_{02}}. \tag{36b}$$

Equations (36) indicate that the position of the second zone plate ZP_2 must be at the front focal plane of the compensation achromatic lens L_2, and the focal lengths of ZP_2 and ZP_3 must have opposite signs. Now $d(\lambda)$ is also a parabola in λ, given by

$$d(\lambda) = \left(1 - \frac{2}{R_{21}^{1/2}}\right)\frac{(\lambda-\lambda_0)^2}{\lambda_0^2}. \tag{37}$$

Using Eqs. (17) and (37), we find that in order to minimize $|A(\lambda)|$ [alternatively $|a(\lambda)|$] and $|d(\lambda)|$ simultaneously, it is best to let $|f_{01}|=|f_{02}|$. Both $|d(\lambda)|$ and $|a(\lambda)|$ have the same maximum, 0.0738, at the two ends of the visible range.

The combination of a refractive achromatic lens and a zone plate can also be used to correct directly the quadratic phase factor at the output plane of the higher-order imperfect achromatic Fourier transformer, which is shown in Fig. 5. Here we require $d(\lambda)$ to be equal to zero at three different wavelengths, as

$$d(\lambda)|_{\lambda=\lambda_m} = 0, \quad m = 1,2,3. \tag{38}$$

Solving Eq. (38), we find that the focal length of achromatic lens L_2 is still equal to the distance z_4, but the focal length of the third zone plate ZP_3 is

$$f_{03} = -\frac{1.56583 z_4^2}{f_{02}}. \tag{39}$$

Equation (39) indicates that the focal length of ZP_3 has the opposite sign to that of ZP_2.

5 Achromatic Optical Fourier Processors

By cascading two perfect achromatic Fourier transformers, it is possible to obtain an achromatic optical Fourier processor. With such a processor, we can perform optical correlation and spatial filtering with a broadband light source. Basically, the achromatic Fourier processor is a white-light imaging system, whose Wigner matrix is characterized by its elements $B=C=0$, while A represents the wavelength-independent total imaging magnification. The filtering plane is the output plane of the first achromatic Fourier transformer. Since in most cases we only detect the intensity at the output plane of an imaging system, the requirements reduce to $B=0$ and $A(\lambda)=$ constant. The coefficient C only affects the quadratic phase factor at the image plane. Then the second achromatic Fourier transformer could be an imperfect achromatic Fourier transformer, which simplifies the design constraints.

Another approach to obtain an achromatic Fourier processor is an inverse procedure. First, we devise a wavelength-independent imaging system. Then the filtering plane is selected by requiring the Wigner matrix generated by the components before the filtering plane to be of some special form. Specifically, the coordinate transformation represented by this Wigner matrix must be a rotation by 90 deg combined with arbitrary shear in the v direction only.

A possible optical processor setup in which a perfect achromatic Fourier transformer is cascaded with an imperfect achromatic Fourier transformer (where $z_1=z_2=0$) is shown in Fig. 8. Figure 8(a) is the direct expanded version, where the incident beam is a plane wave and the needed filter located between the two Fourier transformers. The achromatic lenses L_2 and L_3 and the zone plates ZP_3 and ZP_4 are all located at the same plane (filter plane). In order

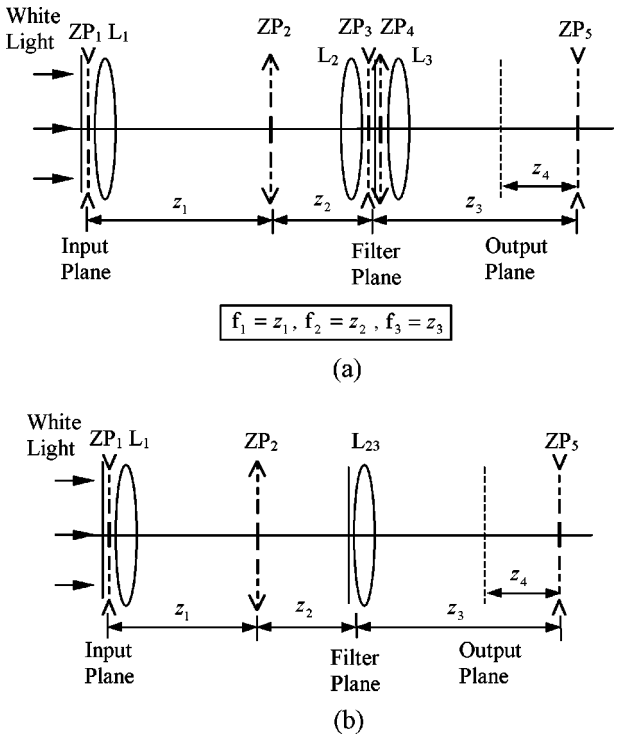

Fig. 8 Setup of an achromatic Fourier processor by cascading two achromatic Fourier transformers, to first-order approximation: (a) expanded version, (b) compact version.

to make the optical setup more compact, it is possible to combine L_2 and L_3 into one lens L_{23} with a focal length f_{23}, and to let ZP_3 and ZP_4 cancel each other, which means $f_{04}=-f_{03}$. Then, the setup evolves into the compact setup shown in Fig. 8(b), where the final output image is virtual. It is possible to obtain the focal length f_{05} of ZP_5 and the focal length f_{23} of the combined lens L_{23}, by using Eqs. (16a) and (36b). The results are

$$f_{05}=-(M_{23})^2 f_{02}, \tag{40}$$

$$\frac{1}{f_{23}}=\frac{1}{z_2}+\frac{1}{z_3}, \tag{41}$$

where $M_{23}=z_3/z_2$. Equation (41) indicates that ZP_2 and ZP_5 are located at conjugate planes.

Since the lens L_1 and the zone plate ZP_1 at the input plane do not affect the imaging properties of the overall setup in the sense of intensity, then the three remaining optical components ZP_2, L_{23}, and ZP_5 can be viewed together as the wavelength-independent imaging part of the setup. This imaging part of the setup is a particular case of the general three-lens configuration proposed by Faklis and Morris[11] and then studied by Tajahuerce et al.[19] Under the constraints in Eqs. (40) and (41), the action of ZP_2 in this three-component wavelength-independent imaging part of the setup is canceled by ZP_5 and the achromatic lens L_{23}. Thus, this imaging part of the setup is exactly equivalent to the single achromatic lens (L_{23}) imaging setup.

The same results as above can be derived by requiring the elements of the Wigner matrix of the three-component setup to satisfy the exact imaging conditions as

$$B(\lambda)=0, \tag{42a}$$

$$\frac{\partial A(\lambda)}{\partial \lambda}=\frac{\partial D(\lambda)}{\partial \lambda}=0, \tag{42b}$$

where the total Wigner matrix does not include the effects of the lens L_1 and the zone plate ZP_1. Then, solving Eq. (42) together with Eq. (41) yields

$$A(\lambda)=-\frac{f_{23}}{z_1+z_2-f_{23}}=-M_0, \tag{43a}$$

$$D(\lambda)=\frac{1}{A(\lambda)}, \tag{43b}$$

$$z_4=-\frac{z_1 f_{23}^2}{(z_2-f_{23})(z_1+z_2-f_{23})}=-M_{23}M_0 z_1, \tag{43c}$$

and the relation in Eq. (40), where M_0 is the lateral magnification between the input plane and the output image plane by the lens L_{23}.

Equations (44) indicate that the total magnification $A(\lambda)$ of the system and the final image position z_4 are completely wavelength-independent. Also, the relations in Eqs. (40) and (41) are valid independently of the position of the object along the optical axis. Thus, by changing the object distance z_1, and correspondingly changing the focal length f_1 of the lens L_1 and f_{01} of the zone plate ZP_1, we can move the filter plane from the plane adjacent to the lens L_{23} to any position between ZP_2 and L_{23}. The relative scaling error in the filter plane is fixed, according to Eq. (19), but any change of z_1, f_1, and f_{01} will also change the required resolution of the filter, the total magnification, and the position of the final image plane. Furthermore, we note that, for the compact setup in Fig. 8(b), the achromatic Fourier transformation at the filter plane is imperfect, containing a quadratic phase factor. This may degrade the output results.

In a similar way, we can cascade the second-order perfect achromatic Fourier transformer with another second-order imperfect achromatic Fourier transformer to achieve an exact achromatic imaging system with a negligible relative scaling error at the filter plane.

Finally, we note that the optical setup in Fig. 8(b) could serve as an achromatic Fourier transform setup when the input object is just a point object (very small pinhole). As a result, it is possible to remove all the lenses (refractive and diffractive) at the input plane without affecting the Fourier transformation. The reason is that, if the complex amplitude of the point object $u(x)$ is taken as the delta function $\delta(x)$, then the complex amplitude at the input plane is not changed, regardless of whether there are lenses at the input plane or not. This can be written as

$$u(x)\exp\left(-j\frac{\pi}{\lambda F}x^2\right)=\delta(x)\exp\left(-j\frac{\pi}{\lambda F}x^2\right)=\delta(x), \tag{44}$$

where F is the equivalent focal length of the combination of all the lenses at the input plane. Then the Fourier transform setup becomes simple; it was studied by Lancis et al.[33] Specifically, the image at the output plane of the setup will be the Fourier transform pattern of the filter. Such a Fourier transform setup has the advantage that, for each wavelength, the Fourier transform pattern is located exactly at a plane that is the conjugate plane of the point-object plane but with a wavelength-dependent scaling factor and a wavelength-dependent quadratic phase factor. In our notation, the scaling factor of the Fourier transformation is the second element of the Wigner matrix which describes the sub-setup between the filter plane and the output Fourier transform plane.

6 Concluding Remarks

The conventional design of optical transformers and processing systems that use polychromatic light usually involves tedious and error-prone Fresnel diffraction calculations, in order to compensate for the inherent chromatic dispersion. In this paper, we present a new design procedure, based on Wigner matrix algebra, which provides a better insight into what is needed for achromatization. With this design procedure, which is useful for geometrical as well as physical optics, any wavelength-dependent transformations of the optical system are inherently included. Specific design examples of achromatic Fourier transformers and achromatic optical Fourier processors, to first-order and second-order approximations, have been presented. The design procedure can, of cause, be extended to many other optical systems that exploit polychromatic light.

Acknowledgments

This work was supported in part by the Albert Einstein Minerva Center for Theoretical Physics. Dayong Wang's permanent address is the Department of Applied Physics, Beijing Polytechnic University, Beijing 100022, China. Adolf W. Lohmann's permanent address is the Laboratory für Nachrichtentechnik, Erlangen-Nürnberg University, Cauerstraße 7, D-91058 Erlangen, Germany.

References

1. R. H. Katyl, ''Compensating optical systems. Part 3: Achromatic Fourier transformation,'' *Appl. Opt.* **11**(5), 1255–1260 (1972).
2. S. J. Bennett, ''Achromatic combination of hologram optical elements,'' *Appl. Opt.* **15**(2), 542–545 (1976).
3. E. N. Leith and G. J. Swanson, ''Achromatic interferometers for white light optical optical processing and holography,'' *Appl. Opt.* **19**(4), 638–644 (1980).
4. G. M. Morris and N. George, ''Space and wavelength dependence of a dispersion-compensented matched filter,'' *Appl. Opt.* **19**(22), 3843–3850 (1980).
5. G. M. Morris, ''Diffraction theory for an achromatic Fourier transformation,'' *Appl. Opt.* **20**(11), 2017–2025 (1981).
6. G. M. Morris, ''An ideal achromatic Fourier processor,'' *Opt. Commun.* **39**(3), 143–147 (1981).
7. G. D. Collins, ''Achromatic Fourier transform holography,'' *Appl. Opt.* **20**(18), 3109–3119 (1981).
8. R. Ferriere and J. P. Goedgebuer, ''Achromatic system for far-field diffraction with broadband illumination,'' *Appl. Opt.* **22**(10), 1540–1545 (1983).
9. S. Leon and E. N. Leith, ''Optical processing and holography with polychromatic point source illumination,'' *Appl. Opt.* **24**(21), 3638–3642 (1985).
10. F. T. S. Yu, ''Principles of optical processing with partially coherent light,'' in *Progress in Optics*, E. Wolf, Ed., Vol. 16, pp. 221–275, North-Holland, London (1986).
11. D. Faklis and G. M. Morris, ''Broadband imaging with holographic lenses,'' *Opt. Eng. (Bellingham)* **28**(6), 592–598 (1989).
12. P. Andrés, J. Lancis, and W. D. Furlan, ''White-light Fourier transformer with low chromatic aberration,'' *Appl. Opt.* **31**(23), 4682–4687 (1992).
13. J. Lancis, P. Andrés, W. D. Furlan, and A. Pons, ''All-diffractive achromatic Fourier transform setup,'' *Opt. Lett.* **19**(6), 402–404 (1994).
14. J. Lancis, E. E. Sicre, A. Pons, and G. Saavedra, ''Achromatic white-light self-imaging phenomenon: an approach using the Wigner distribution function,'' *J. Mod. Opt.* **42**(2), 425–434 (1995).
15. C. L. Adler, W. S. Rabinovich, S. R. Bowman, B. J. Feldman, D. S. Katzer, and C. S. Kyono, ''Dynamic white light holography using an optically addressed multiple quantum well spatial light modulator,'' *Opt. Commun.* **114**, 375–380 (1995).
16. J. Lancis, E. Tajahuerce, P. Andrés, V. Climent, and E. Tepichín, ''Single-zone-plate achromatic Fresnel-transform setup: pattern tunability,'' *Opt. Commun.* **136**, 297–305 (1997).
17. F. T. S. Yu, ''Exploitation of incoherent source for partially coherent processing,'' *Opt. Eng. (Bellingham)* **36**(5), 1458–1464 (1997).
18. E. Tajahuerce, V. Climent, J. Lancis, M. Fernández-Alonso, and P. Andrés, ''Achromatic Fourier transforming properties of a separated diffractive lens doublet: theory and experiment,'' *Appl. Opt.* **37**(26), 6164–6173 (1998).
19. E. Tajahuerce, J. Lancis, V. Climent, and P. Andrés, ''Hybrid (refractive-diffractive) Fourier processor: a novel optical architecture for achromatic processing with broadband point-source illumination,'' *Opt. Commun.* **151**, 86–92 (1998).
20. P. Andrés, V. Climent, J. Lancis, G. Minguez-Vega, E. Tajahuerce, and A. W. Lohmann, ''All-incoherent dispersion-compensated optical correlator,'' *Opt. Lett.* **24**(19), 1331–1333 (1999).
21. A. Pe'er, D. Wang, A. W. Lohmann, and A. A. Friesem, ''Optical correlation with totally incoherent light,'' *Opt. Lett.* **24**(21), 1469–1471 (1999).
22. M. J. Bastiaans, ''The Wigner distribution function applied to optical signals and systems,'' *Opt. Commun.* **25**(1), 26–30 (1978).
23. M. J. Bastiaans, ''Wigner distribution function and its application to first-order optics,'' *J. Opt. Soc. Am.* **69**(12), 1710–1716 (1979).
24. D. Dragoman, ''The Wigner distribution function in optics and optoelectronics,'' in *Progress in Optics*, E. Wolf, Ed., Vol. 37, pp. 1–56, North-Holland, London (1997).
25. A. W. Lohmann, ''Image rotation, Wigner rotation, and the fractional Fourier transform,'' *J. Opt. Soc. Am. A* **10**(10), 2181–2186 (1993).
26. A. W. Lohmann, D. Mendlovic, and Z. Zalevsky, ''Fractional transformations in optics,'' in *Progress in Optics*, E. Wolf, Ed., Vol. 38, pp. 263–342, North-Holland, London (1998).
27. M. Nazarathy and J. Shamir, ''First-order optics—a canonical operator representation: lossless systems,'' *J. Opt. Soc. Am.* **72**(3), 356–364 (1982).
28. A. E. Siegman, ''Complex paraxial wave optics,'' Chap. 20 in *Lasers*, pp. 777–814, University Science Books, Mill Valley, CA (1986).
29. J. Shamir and N. Cohen, ''Root and power transformations in optics,'' *J. Opt. Soc. Am. A* **12**(11), 2415–2423 (1995).
30. T. Alieva and F. Agullo-Lopez, ''Imaging in first-order optical systems,'' *J. Opt. Soc. Am. A* **13**(12), 2375–2380 (1996).
31. A. Sahin, H. M. Ozaktas, and D. Mendloviic, ''Optical implementations of two-dimensional fractional Fourier transforms and linear canonical transforms with arbitrary parameters,'' *Appl. Opt.* **37**(11), 2130–2141 (1998).
32. K. B. Wolf, ''Construction and properties of canonical transforms,'' Chap. 9 in *Integral Transforms in Science and Engineering*, pp. 381–416, Plenum Press, New York (1979).
33. J. Lancis, E. Tajahuerce, P. Andrés, G. Mínguez-Vega, M. Fernández-Alonso, and V. Climent, ''Quasi-wavelength-independent broadband optical Fourier transformer,'' *Opt. Commun.* **172**, 153–160 (1999).

Dayong Wang received his BS degree in optical engineering in 1989 from Huazhong University of Science and Technology, Wuhan, China, and his PhD degree in physics in 1994 from Xian Institute of Optics and Fine Mechanics, Chinese Academy of Science, China. He is currently a postdoctoral research fellow with the Weizmann Institute of Science in Israel. His research interests include optical signal processing, optical storage, and diffractive optical elements.

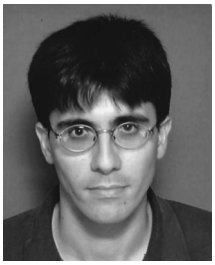

Avi Pe'er received his BSc in physics and computer science from the University of Tel-Aviv, Israel, in 1996, and his MSc in physics from the Weizmann Institute of Science, Israel, in 1999. He is now a PhD student in the Department of Physics of Complex Systems at the Weizmann Institute of Science. His research interests are in the fields of optical processing and holography with incoherent light.

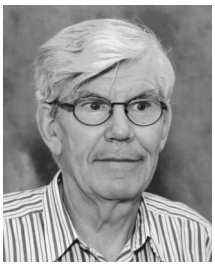

Adolf W. Lohmann studied at the University of Hamburg, Germany, until he received the PhD degree in 1953. His locations since 1953 have been Braunschweig (Germany), Stockholm, San Jose (California), San Diego (California), and Erlangen (Germany). After retirement in 1992 he was involved in research activities in Israel (Weizmann Institute of Science and Tel Aviv University) and in Mexico (INAOE). He was president of the International Commission for Optics (1978–1981). He is interested in optical information processing, including computer holography, optical interconnects, transformations in optics, and superresolution.

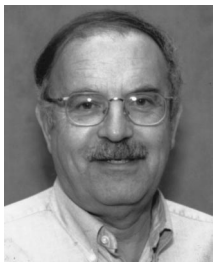

Asher A. Friesem received the BSc and PhD degrees from the University of Michigan, Ann Arbor, in 1958 and 1968, respectively. From 1958 to 1963 he was employed by Bell Aero Systems Company and Bendix Research Laboratories. From 1963 to 1969, he was at the University of Michigan Institute of Science and Technology, conducting investigations in coherent optics, mainly in the areas of optical data processing and holography. From 1969 to 1973 he was the principal research engineer in the Electro-Optics Center of Harris, Inc., performing research in the areas of optical memories and displays. In 1973, he joined the staff of the Weizmann Institute of Science, Israel, becoming a professor of optical sciences in 1977. He is concerned with new holographic concepts and applications, optical image processing, and electro-optics devices. Dr. Friesem is a fellow of the Optical Society of America, a fellow of the IEEE, Vice President of the International Commission for Optics, chairman of the Israel Laser and Electro-Optics Society, and a member of SPIE.